ELSEVIER

Chemical Physics 217 (1997) 167–178

Chemical Physics

Dissipative tunneling with periodic polychromatic driving: Exact results and tractable approximations

Milena Grifoni, Ludwig Hartmann, Peter Hänggi *

Institut für Physik, Universität Augsburg, Memminger Strasse 6, 86135 Augsburg, Germany

Received 17 October 1996

Abstract

We investigate the long-time dynamics in dissipative two-level-systems (TLS) when driven by – monochromatic or pulse-shaped – periodic fields. The environmental influence is investigated within the noninteracting-blip appoximation (NIBA), while no restrictions are assumed on the driving force. With the focus being on electron-transfer (ET) reactions in condensed media, we consider a continuous Ohmic spectrum for the bath modes. The asymptotic dynamics exhibits always the periodicity of the external force. The induced oscillations show a smooth periodic behavior which becomes richer, if, for example, multiphoton resonances occur. For monochromatic driving, the oscillatory multiresonance pattern becomes gradually smoothed out when the temperature, and/or the Ohmic strength are sufficiently high. It may persist, however, for pulse-shaped driving. Exact NIBA analytical and/or numerical solutions, for both the Ohmic transfer rate and for the driven dynamics, are used to determine the validity range of the short-time approximation for the bath correlation functions. The latter is frequently employed to investigate the ET dynamics. Our analysis shows that the short-time approximation may give qualitative incorrect results at low temperatures. © 1997 Elsevier Science B.V.

1. Introduction

The model of a two-level system coupled to a thermal bath has been successfully applied to describe diverse phenomena occurring in physical and chemical systems. It can describe, for example, hydrogen tunneling in condensed media [1], tunneling of atoms between an atomic-force microscope tip and a surface [2], or of the magnetic flux in a superconducting quantum interference device (SQUID) [3]. Since the seminal works by Marcus [4] and Levich [5] this same model has been applied to describe nonadiabatic chemical reactions in the condensed phase, i.e., electron transfer (ET) [6–10] or proton transfer reactions [11].

This two-level-system (TLS), when isolated from the thermal bath, is the simplest system exhibiting quantum interference effects, as it can be prepared to oscillate clockwise between the eigenstates in the left and right well. Quite generally, the stochastic influence results in a reduction of the coherent tunneling motion by incoherent processes [12–14], and may even lead to a transition to localization at zero temperature [15]. An important question is to which degree the TLS dynamics is influenced by externally applied time-dependent fields [16–29]. In particular, in the absence of interaction with a bath, a complete destruction of tunneling can be induced by a coherent driving field of appropriate frequency and strength [16]. This effect can be stabilized in the presence of dissipation

* Corresponding author.

PII S0301-0104(97)00020-7

[17,20]. The possibility to control a-priori the proton transfer by an electric field has been first addressed in [18] in the classical limit. This same issue applied to the case of ET transfer rate in a polar solvent was subsequently discussed in [21]. Long-time coherent oscillations may arise due to driving induced correlations between tunneling transitions [19,22,23,27]. This oscillatory behavior has previously not been detected in [20], due to the fast field approximation used in the analytic treatment of the driven dynamics. Finally, other interesting examples of control of the TLS dynamics are the enhancement of the TLS response to a weak coherent signal [26], i.e., quantum stochastic resonance, or of the periodic asymptotic tunneling amplitude [27], for optimal values of the stochastic forces. The possibility of inversion of the population between the donor and the acceptor in an ET process has been recently discussed in [21,28]. Moreover, novel effects, such as an exponential enhancement of the transfer rate by an electric field modulating the coupling between the localized states has been addressed recently in [29].

In this work we investigate the possibility of controlling the long-time oscillatory TLS dynamics by a generic periodic field. In particular, we shall address the case of experimental interest of monochromatic and pulse-shaped driving (see Eq. (2) and Fig. 1).

The case of pulse-shaped monochromatic driving has been recently addressed in Ref. [24]. In the approach of Ref. [24], though, the pulse function has not been considered as a continuous periodic function. Put differently, the signal therein has been treated as a sequence of "field-on" time-intervals where known results for fast monochromatic driving could be applied, followed by "field-off" intervals, where, on the contrary, results for the static transfer rates were used.

For monochromatic driving, it is found that the asymptotic periodic electronic population may exhibit multi-resonance peaks when the driving frequency is an integer submultiple of the asymmetry energy between the localized states. This phenomenon may be interpreted as a multiphoton absorption or emission process at the proper frequencies of the TLS. It should be observable in ET reactions in nonpolar media at sufficiently low temperatures and small reorganization energies. On the other hand, for ET in polar media the reorganization energy is always too large for this fine structure to be visible.

For pulse-shaped driving, the periodic dynamics exhibits again an oscillatory behavior on which a fine structure is usually superimposed. Further, as suggested in [24], a pulse-shaped signal might be more appropriate to observe the asymptotic oscillations in ET in polar media. In fact, it is unlikely that the effect of the applied electric field would result in a dielectric breakdown of the solvent due to the very short duration of the pulses.

The paper is organized as follows. In the first part of Section 2 we recall some general results on the dynamics of the periodically driven and dissipative TLS. In the second part of Section 2 some limiting solutions for the case of monochromatic and pulse-shaped driving are discussed. In Section 3 the general results of the previous section are applied to study the asymptotic periodic dynamics, with emphasis put on the ET dynamics in nonpolar media. For this purpose, the bath is assumed to have a continuous spectrum of the Ohmic form. Exact analytical and numerical results for the Ohmic transfer rate and asymptotic dynamics are used to determine the regime of validity of the short-time approximation imposed on the bath correlation functions, which frequently is used in the ET literature. At last, in Section 4, we summarize our findings and draw some conclusions.

2. Tunneling dynamics under periodic driving

The spin-boson Hamiltonian has often been used in the literature to study the dynamics of nonadiabatic ET, or proton-transfer, reactions [8–10,18,21,24,28]. The TLS is associated with electronic basis states that correspond to an electron localized on the donor or on the acceptor site of an ET complex, respectively. The bosonic modes describe the solvent effects, and are assumed to be coupled bilinearly to the TLS coordinates. Taking in addition into account the possibility of an external electric field which couples to the transition dipole moment between the donor and acceptor states, we end up with the time-dependent spin-boson Hamiltonian

$$H(t) = -\frac{\hbar}{2}\left(\Delta\sigma_x + \varepsilon(t)\sigma_z\right) + \frac{1}{2}\sum_i\left(\frac{p_i^2}{m_i} + m_i\omega_i^2 x_i^2 - c_i x_i d\sigma_z\right). \qquad (1)$$

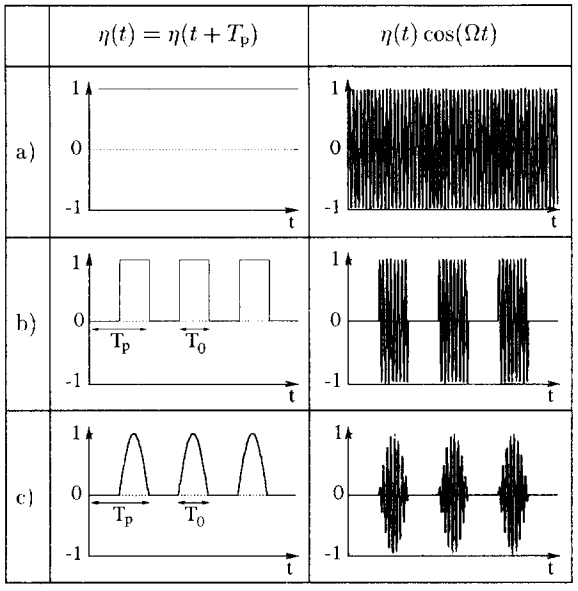

Fig. 1. Different periodic driving signals can be used to control the tunneling dynamics: (a) monochromatic driving; (b) and (c) pulse-shaped polychromatic driving of period T_p. The latter are obtained by modulating a monochromatic signal by a pulse function. T_0 denotes the duration of the pulse.

Here, the σ's are Pauli matrices, and the eigenstates of σ_z are the basis states in a localized representation where d is the tunneling distance between the donor and acceptor localized states. The electronic coupling parameter is given by $\hbar\Delta$, while the asymmetry energy between the two localized positions is $\hbar\varepsilon(t) = \hbar\epsilon_0 + f(t)$. The static part $\hbar\epsilon_0$ represents the bias energy in the absence of the driving field (the reaction heat). The time dependent contribution of the form

$$f(t) = \mu E_0 \eta(t)\cos\Omega t, \qquad \eta(t + T_p) = \eta(t), \quad (2)$$

describes the coupling between the ET system and the external field, where μ is the difference dipole moment between donor and acceptor, and $E_0\cos\Omega t$ is the applied electric field modulated by a periodic function $\eta(t)$ of period $T_p = 2\pi/\Omega_p \geqslant T = 2\pi/\Omega$. Depending on the particular shape of the "pulse" function $\eta(t)$, different experimental realizations may be mimicked as shown in Fig. 1.

Suppose now that at times $t < 0$ the particle is held at the site $\sigma_z = 1$ with the bath prepared at thermal equilibrium at temperature T. We then compute the population difference between the localized states $\langle\sigma_z(t)\rangle \equiv P(t)$ at times $t \geqslant 0$ for this factorizing initial state. After tracing out the thermal bath, all environmental effects are captured by the twice-integrated bath correlation function $Q(t) = Q'(t) + iQ''(t)$ [12,13], where

$$Q(t) = \frac{d^2}{\pi}\int_0^\infty d\omega\,\frac{J(\omega)}{\omega^2}\big(\cosh[\hbar\omega\beta/2] - \cosh[\hbar\omega(\beta/2 - it)]\big)/\sinh[\hbar\omega\beta/2], \quad (3)$$

$\beta = 1/k_BT$, and $J(\omega) = (\pi/2)\sum_i(c_i^2/m_i\omega_i)\delta(\omega - \omega_i)$ is the spectral density of the heat bath. Upon summing over the history of the system's visits of the four states of the reduced density matrix, we can find the exact formal solution for the evolution of a driven damped system in the form of a series in the number of time-ordered tunneling transitions [19,22,23]. Equivalently, as prescribed in Ref. [23], an exact master equation for the population $P(t)$ can be derived. It reads

$$\dot{P}(t) = \int_0^t dt'\,[K^{(-)}(t,t') - K^{(+)}(t,t')P(t')], \quad (4)$$

where the memory kernels $K^{(\pm)}(t,t')$ are defined by a power series in Δ^2. An exact analytical solution of Eq. (4) is known for the special case $\alpha = 1/2$ of the Ohmic friction (see Eq. (22)). For arbitrary Ohmic friction values, or other friction mechanisms, one generally has to resort to approximations. In particular, within the noninteracting-blip approximation (NIBA) [12,13], the kernels in Eq. (4) reduce to the expressions

$$\begin{aligned} K^{(+)}(t,t') &= h^{(+)}(t-t')\cos\zeta(t,t'),\\ K^{(-)}(t,t') &= h^{(-)}(t-t')\sin\zeta(t,t'), \end{aligned} \quad (5)$$

where $\zeta(t,t') = \int_{t'}^t dt''\,\varepsilon(t'')/\hbar$ and

$$\begin{aligned} h^{(+)}(t-t') &= \Delta^2 e^{-Q'(t-t')}\cos[Q''(t-t')],\\ h^{(-)}(t-t') &= \Delta^2 e^{-Q'(t-t')}\sin[Q''(t-t')]. \end{aligned} \quad (6)$$

The NIBA assumes that the average time spent in an off-diagonal state of the reduced density matrix is much smaller than the average time spent in a diagonal state. This assumption is always fulfilled for high

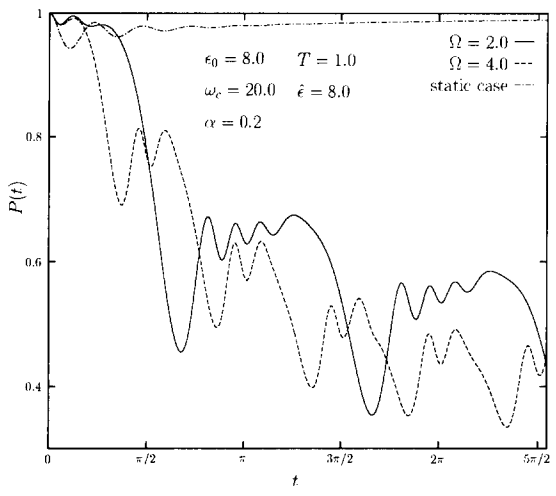

Fig. 2. Large amplitude oscillations in the asymptotic population dynamics described by $P(t)$ induced by a monochromatic field $f(t) = \hbar\hat{\epsilon}\cos\Omega t$ of intermediate frequency Ω. For comparison, the behavior in the absence of driving (static case) is also shown. The fine resonance structure can be interpreted as the result of a multiphoton absorption at the proper frequency of the TLS: The number N of resonances observed satisfies the relation $N = \epsilon_0/\Omega$, where $\hbar\epsilon_0$ is the static asymmetry energy of the TLS. Here and in the following figures, frequencies are in units of $\delta = \Delta/2$, temperatures in units of $\hbar\delta/k_B$ and times in units of δ^{-1}. Moreover, α is the dimensionless Ohmic coupling constant and ω_c the cut-off frequency which characterize the Ohmic spectral density in Eq. (22).

enough friction or high enough temperatures, though the range of validity depends on the specific form chosen for the spectral density $J(\omega)$ of the medium (see also the discussion in Section 3). It is interesting to observe, however, that the polaron transformation approach discussed in [20,21,28] leads, if applied to the Hamiltonian of Eq. (1), to a master equation analogous to Eq. (4) and with kernels identical to Eq. (5). The NIBA then amounts to the Born approximation with respect to the dressed intersite coupling [30]. Eq. (4) is conveniently solved by Laplace transformation. Introducing the Laplace transform $\hat{P}(\lambda) = \int_0^\infty dt\, e^{-\lambda t}P(t)$ of $P(t)$, one obtains

$$\lambda\hat{P}(\lambda) = 1 + \int_0^\infty dt\, e^{-\lambda t}[\hat{K}_\lambda^{(-)}(t) - \hat{K}_\lambda^{(+)}(t)P(t)], \tag{7}$$

where $\hat{K}_\lambda^{(\pm)}(t) = \int_0^\infty dt'\, e^{-\lambda t'}K^{(\pm)}(t+t',t)$. In the absence of driving, the kernels $\hat{K}_\lambda^{(\pm)}$ do not depend on time, and Eq. (7) reproduces well-known results [12,13]. In particular, the TLS dynamics approaches incoherently the stationary equilibrium value $P_{st} = \tanh(\hbar\epsilon_0/2k_BT)$ with relaxation rate $\gamma_0 \equiv \lim_{\lambda,\hat{\epsilon}\to 0}\hat{K}_\lambda^{(\pm)}(t)$ given by

$$\gamma_0 = \int_0^\infty d\tau\, h^{(+)}(\tau)\cos(\tau\epsilon_0). \tag{8}$$

For periodic driving the kernels $\hat{K}_\lambda^{(\pm)}(t)$ have the periodicity of the external field and can be expanded in Fourier series, i.e.,

$$\hat{K}_\lambda^{(\pm)}(t) = \sum_{m=-\infty}^{\infty} k_m^{\pm}(\lambda)e^{-im\Omega_p t}, \tag{9}$$

hence allowing a recursive solution of (7) [22]. In particular, the asymptotic dynamics is determined by the poles of the recursive solution at $\lambda = \pm im\Omega_p$, where m is an integer number. Hence, the asymptotic dynamics is periodic in time with the periodicity $T_p = 2\pi/\Omega_p$ of the driving force, i.e.,

$$\lim_{t\to\infty} P(t) = P^{(as)}(t) = P^{(as)}(t+T_p), \tag{10}$$

satisfying the integro-differential equation

$$\dot{P}^{as}(t) = \mathcal{F}(t) - \frac{\Omega}{2\pi}\int_0^{2\pi/\Omega} dt'\, P^{(as)}(t') \times \mathcal{L}(t', t-t'), \tag{11}$$

which describes the time evolution within a period. Here

$$\mathcal{F}(t) = \sum_n e^{-in\Omega_p t}k_n^-(-in\Omega_p),$$
$$\mathcal{L}(t,t') = \sum_{m,n} e^{-im\Omega_p t}e^{-in\Omega_p t'}k_m^+(-in\Omega_p). \tag{12}$$

This result, within NIBA, is still *exact*. It explicitly shows that also the asymptotic driven dynamics is intrinsically *non-Markovian* and not invariant under continuous time-translations. As shown in Fig. 2 for the case of monochromatic driving $f(t) = \hbar\hat{\epsilon}\cos\Omega t$,

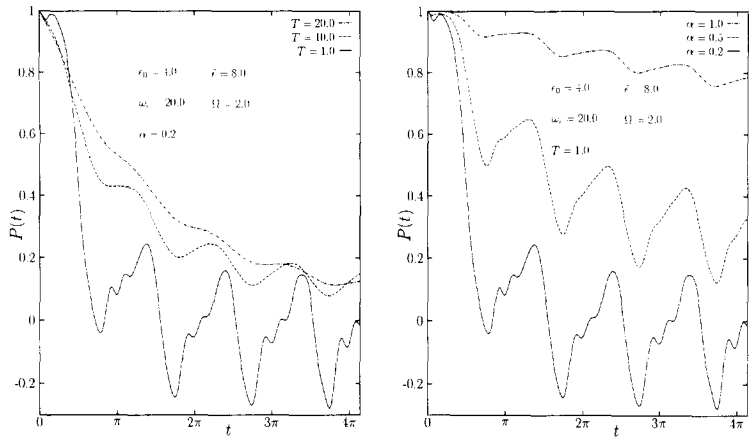

Fig. 3. The oscillatory asymptotic dynamics of the population $P(t)$ induced by a monochromatic field $f(t) = \hbar\hat{\epsilon}\cos\Omega t$ is smoothed out as the temperature T (left panel) or the Ohmic coupling strength α (right panel) increases.

($\hbar\hat{\epsilon} \equiv \mu E_0$ and $\eta(t) = 1$), driving-induced correlations may lead, for example, to large amplitude oscillations in the asymptotic dynamics. Moreover, a fine resonance structure may be superimposed to the oscillatory behaviour. For large asymmetries ϵ_0 the number N of resonances is given by the ratio $N = \epsilon_0/\Omega$. This phenomenon may be interpreted as a multiphoton absorption or emission process at the proper frequencies of the TLS. In Fig. 2, as in the other figures, the bath is assumed to have an *Ohmic spectrum* as given in Eq. (22). Moreover, in all of our figures frequencies are given in units of $\delta \equiv \Delta/2$, temperatures in units of $\hbar\delta/k_B$ and times in units of δ^{-1}. Here, $\hbar\delta$ represents half of the coupling energy between the localized electronic states. If for example, as in Section 3, these general results are applied to describe the ET dynamics in condensed media, the half energy $\hbar\delta$ can be taken to be $1\,\mathrm{cm}^{-1}$ (so that $\hbar\delta/k_B \simeq 1.44$ K and $\delta^{-1} \simeq 33$ ps). The coherent oscillatory behaviour is depicted also in Fig. 3, where the effect of temperature and friction is investigated. It is shown that the driving-induced coherent oscillations are smoothed out by bath-induced incoherent transitions as the temperature or the coupling strength are increased.

As shown by Eq. (4) or Eqs. (7) and (11) the transient, as well as the long-time dynamics, depends on an intriguing interplay between the stochastic and driving forces. Though, as discussed below and as depicted in Figs. 4 and 5 for the case of monochromatic and pulse-shaped driving, respectively, when a separation of time scales is possible, Markovian approximations to the exact NIBA solutions can be invoked.

2.1. Monochromatic driving

Before considering the case of periodic pulse-shaped driving of the form $f(t) = \hbar\hat{\epsilon}\eta(t)\cos\Omega t$, it is instructive to discuss some approximations to the dynamics in the presence of monochromatic driving (i.e., $\eta(t) = 1$ in Eq. (2) and hence Ω equals Ω_p). For a more extensive discussion we refer to previously published works quoted below. In the following we shall restrict to the low and high frequency regimes $\Omega_p \gg \tau_K^{-1}$ and $\Omega_p \ll \tau_K^{-1}$, respectively. Here, τ_K is the characteristic memory time of the kernels of Eq. (5) and depends on the specific characteristics of the medium (see Section 4).

2.1.1. Low frequency driving

As discussed above, an analysis of the poles of the exact NIBA equation (7) reveals that the long-time dynamics is dominated by the poles of $\hat{P}(\lambda)$ in $\lambda = \pm im\Omega_p$ (with m an integer number), leading to the integro-differential equation (11) for the asymptotic periodic dynamics. Hence, to leading order, in the low frequency regime $\Omega_p \ll \tau_K^{-1}$, the λ dependence of the kernels $\hat{K}_\lambda^{(\pm)}(t)$ can be neglected, if only the long-time behavior is of interest. In other words, the driving field is slow enough that driving-induced non-Markovian correlations do not contribute

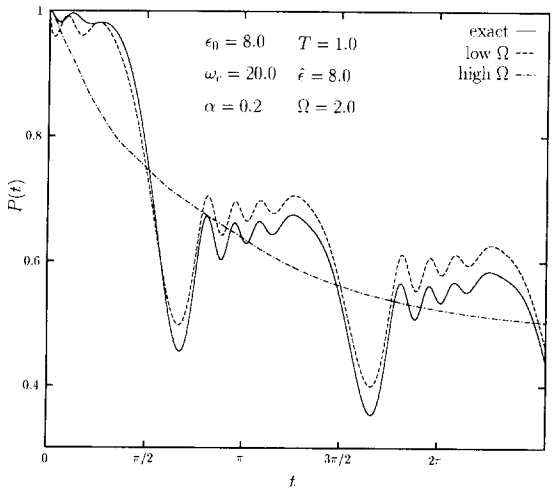

Fig. 4. The figure shows a comparison between the prediction of the exact NIBA equation (4) for the electronic population $P(t)$ with the low-frequency and high-frequency approximations Eqs. (13) and (17), respectively. A monochromatic driving field $f(t) = \hbar\hat{\epsilon}\cos\Omega t$ of intermediate frequency Ω is used.

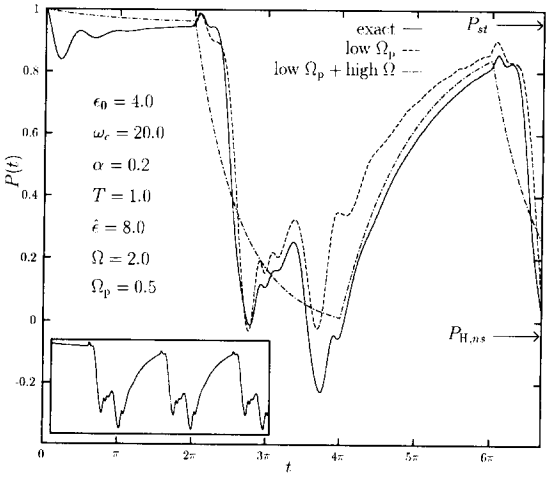

Fig. 5. Dynamics of the electronic population $P(t)$ induced by periodic pulses as in Fig. 1(b). A low frequency periodic square pulse of period $T_p = 2\pi/\Omega_p$ and pulse duration $T_0 = T_p/2$ is multiplied by a monochromatic signal of intermediate frequency Ω. The oscillatory dynamics is depicted in the inset where $P(t)$ is plotted for a longer time. The prediction of the low frequency approximation Eq. (13) and that of Eq. (20) (valid for slow pulses with internal high frequency oscillations) is also shown. The low Ω_p-high Ω approximation describes the TLS oscillations between the two bounds P_{st} and $P_{H,ns}$ indicated by the arrows. This approximation misses the fine structure due to the monochromatic component of the driving. See also Fig. 3.

[19,22]. The *long-time* dynamics, within the NIBA, is intrinsically incoherent and the low frequency approximation $P_L(t)$ to $P(t)$ obeys the rate equation

$$\dot{P}_L(t) = -\gamma_L(t)[P_L(t) - P_{L,ns}(t)], \tag{13}$$

with low frequency rate $\gamma_L(t) \equiv \lim_{\lambda\to 0}\hat{K}_\lambda^{(+)}(t)$ given by

$$\gamma_L(t) = \int_0^\infty d\tau\, h^{(+)}(\tau)\cos[\zeta(t+\tau,t)], \tag{14}$$

and time-dependent, nonstationary equilibrium value $P_{L,ns}(t) = \rho_L(t)/\gamma_L(t)$, where

$$\rho_L(t) = \int_0^\infty d\tau\, h^{(-)}(\tau)\sin[\zeta(t+\tau,t)]. \tag{15}$$

Eq. (13) is easily solved in terms of quadratures [19,22]. In the limit $\Omega \to 0$, one obtains that $\zeta(t, t-\tau) \to \tau\varepsilon(t)$ and $P_{ns,L}(t) \to \tanh\hbar\beta\varepsilon(t)/2$, so that $\varepsilon(t)$ behaves like a time dependent asymmetry, and an adiabatic detailed balance condition is fulfilled in analogy with the static case. In general, however, the detailed balance condition does not hold true in the presence of driving. In the limit $\hat{\epsilon} \to 0$ the low frequency rate $\gamma_L(t)$ reduces to the static rate γ_0 in Eq. (8). In Fig. 4 the predictions of the low frequency approximation given by Eq. (13) are compared with those of the exact NIBA equation (4) for the case of moderately small Ohmic friction (see Eq. (22)). The predictions of the high frequency approximation discussed in the next subsection are also reported.

2.1.2. *High frequency regime*

In the high frequency regime $\Omega_p \gg \tau_K^{-1}$, the driving field oscillates too fast to account for the details of the dynamics within one period. Hence, a good approximation to the true dynamics described by Eq. (4) amounts to approximate the kernels $K^{\pm}(t,t')$ in Eq. (4) with their average $\langle K^{(\pm)}(t,t')\rangle_{T_p} \equiv K_0^{(\pm)}(t-t')$ over a period (or $\hat{K}_\lambda^{(\pm)}(t)$ in Eq. (7) with their average $k_0^{\pm}(\lambda)$ given by the term with $m = 0$ in Eq. (9)). Hence, the essential dynamics of $P(t)$ is described by $\langle P(t)\rangle_{T_p} \equiv P_H(t)$ [21–23,28]. The evaluation of the time-averaged kernels is in turn readily accomplished by noticing that this average

has only to be carried out on the field dependent contributions $\cos\zeta(t,t')$ and $\sin\zeta(t,t')$. One obtains

$$\begin{aligned}\langle\cos\zeta(t,t')\rangle_{T_p} &= J_0\Big(\frac{2\hat{\epsilon}}{\Omega_p}\sin\frac{\Omega_p(t-t')}{2}\Big)\cos\epsilon_0(t-t'),\\ \langle\sin\zeta(t,t')\rangle_{T_p} &= J_0\Big(\frac{2\hat{\epsilon}}{\Omega_p}\sin\frac{\Omega_p(t-t')}{2}\Big)\sin\epsilon_0(t-t'),\end{aligned} \tag{16}$$

where $J_0(z)$ is the zero order Bessel function of first kind. Hence, time translation invariance has been recovered by the averaging procedure, and the resulting equation for $P_H(t)$ obtained from Eq. (4) is now of *convolutive* form. From Eq. (7) one obtains $\hat{P}_H(\lambda) = [1+k_0^-(\lambda)/\lambda]/[\lambda+k_0^+(\lambda)]$. Thus, a fast field suppresses the periodic long-time oscillations, and [as follows approximating $k_0^{\pm}(\lambda)\simeq k_0^{\pm}(0)$] the TLS satisfies at *long times* the rate equation

$$\dot{P}_H(t) = -\gamma_H[P_H(t)-P_{H,ns}], \tag{17}$$

where $P_{H,ns} = k_0^-(0)/k_0^+(0)$ is the averaged nonstationary equilibrium value at high frequencies. The high frequency relaxation rate $k_0^+(0)\equiv\gamma_H$ is given by

$$\gamma_H = \int_0^\infty d\tau\, h^{(+)}(\tau)\cos(\tau\epsilon_0)J_0\Big(\frac{2\hat{\epsilon}}{\Omega}\sin\frac{\Omega\tau}{2}\Big). \tag{18}$$

In the limit $\hat{\epsilon}\to 0$ the modified rate γ_H reduces to the static one γ_0 of Eq. (8).

Hence, from Eqs. (13) and (17) we may conclude that, both for low and high frequency monochromatic driving, the long-time behavior obeys within a good approximation a Markovian dynamics. The oscillatory asymptotic tunneling dynamics under pulse-shaped driving is addressed in more detail in the next subsection.

2.2. Pulse-shaped periodic driving

Due to the results obtained in the previous section, we have all the necessary tools to discuss the case of pulse-shaped periodic driving of the form $f(t) = \hbar\hat{\epsilon}\eta(t)\cos\Omega t$.

Because Eqs. (13) and (17) are restricted only by the assumption of a separation of time scales, in the parameter regimes $\tau_K^{-1}\gg\Omega_p$ or $\tau_K^{-1}\ll\Omega_p$ the same reasoning as for the case of low frequency or high frequency monochromatic driving, respectively, holds true. The dynamics will then be approximated by Eq. (13) or by Eq. (17) with the appropriate high frequency relaxation rate as it emerges from the averaging procedure. Though, because the resulting dynamics is Markovian, an approximation to Eq. (13) can in addition be discussed in the parameter regime $\Omega\gg\tau_K^{-1}\gg\Omega_p$. That is, we assume that the pulse-shape function $\eta(t)$ is a slowly varying function on the time scale set by the memory of the kernels in Eq. (5), while, on the contrary, the monochromatic part $\cos\Omega t$ is fastly changing. Although the oscillatory long-time dynamics will assume the periodicity of the slow pulse shape function $\eta(t)$ (see Eq. (10)), the dynamics within a pulse period T_p is also determined by the fast monochromatic signal. Hence, due to the assumption $\Omega\gg\tau_K^{-1}$, a good approximation to Eq. (13) can be obtained by performing the average $\langle P_L(t)\rangle_T$ of $P_L(t)$ over the fastly oscillating field. The average over the period $T = 2\pi/\Omega$ yields [1]

$$\begin{aligned}\langle\cos\zeta(t,t')\rangle_T &= J_0\Big(\frac{2\hat{\epsilon}\eta(t)}{\Omega}\sin\frac{\Omega(t-t')}{2}\Big)\cos\epsilon_0(t-t'),\\ \langle\sin\zeta(t,t')\rangle_T &= J_0\Big(\frac{2\hat{\epsilon}\eta(t)}{\Omega}\sin\frac{\Omega(t-t')}{2}\Big)\sin\epsilon_0(t-t'),\end{aligned} \tag{19}$$

and the smooth, slowly oscillating function $\langle P_L(t)\rangle_T$ satisfies the rate equation (13) with relaxation rate

$$\gamma_{L,\eta}(t) = \int_0^\infty d\tau\, h^{(+)}(\tau) \times J_0\Big(\frac{2\hat{\epsilon}\eta(t)}{\Omega}\sin\frac{\Omega\tau}{2}\Big)\cos(\tau\epsilon_0), \tag{20}$$

and a nonstationary asymptotic value $P_{ns,\eta}(t) = \rho_{L,\eta}(t)/\gamma_{L,\eta}(t)$, where

$$\rho_{L,\eta}(t) = \int_0^\infty d\tau\, h^{(-)}(\tau) \times J_0\Big(\frac{2\hat{\epsilon}\eta(t)}{\Omega}\sin\frac{\Omega\tau}{2}\Big)\sin(\tau\epsilon_0). \tag{21}$$

[1] A similar approximation has recently been discussed in Ref. [25] for the case of bichromatic driving.

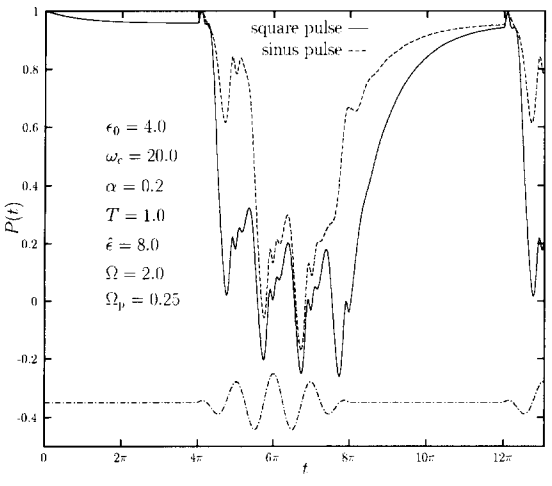

Fig. 6. Oscillatory dynamics for the *ET* population $P(t)$ induced by the two different periodic polychromatic functions in Fig. 1(b) and Fig. 1(c). $T_p = 2\pi/\Omega_p$ denotes the period of the periodic pulse, $T_0 = T_p/2$ the pulse duration and Ω the frequency of the monochromatic signal. The dot-dashed curve at the bottom of the figure shows for the reader's convenience the pulse signal of Fig. 1(c). The sinus-like pulse gives rise to a different fine structure, as compared to the square pulse. The differences occur both at the beginning an at the end of the individual pulse. In the middle of the pulse, the two signals have almost the same amplitudes and the differences become only quantitative.

Note that when $\eta(t) = 1$, the high frequency approximation (17) is recovered. This is in agreement with the physical intuition saying that a monochromatic signal can be thought to be a pulse-shaped signal with an infinite pulse period T_p. The asymptotic oscillatory dynamics for the case of Ohmic friction and pulse-shaped driving of the type (b) is shown in Fig. 5. For comparison, the prediction of the rate equation Eq. (13) with Eqs. (14) and (15), is also depicted. In addition, is reported the prediction of Eq. (13) where the approximated equations (20) and (21), obtained in the limit of low Ω_p and high Ω, are used. This latter low Ω_p-high Ω approximation describes the TLS oscillations between the two bounding values $P_{st} \equiv P_{ns,\eta=0}$ and $P_{H,ns} \equiv P_{ns,\eta=1}$. These bounds are indicated by the arrows in Fig. 5. The low Ω_p-high Ω approximation scheme misses the fine structure due to the monochromatic driving.

The comparison between pulse-shaped driving of the type (b) and (c) in Fig. 1 is shown in Fig. 6. The two different pulse functions do not show a big qualitative difference.

3. Asymptotic ET dynamics

In order to make quantitative predictions on the ET dynamics, we next specify a form for the spectral density $J(\omega)$ of the bath that is suitable to describe ET reactions. In the ET literature, different kinds of frequency dependence for the spectral density $J(\omega)$ have been used. For the case of long-range ET in molecular solids (e.g., in proteins) a suitable spectral function can be chosen to be of the Ohmic form [28], where

$$J(\omega) = \frac{2\pi\hbar}{d^2}\alpha\omega e^{-\omega/\omega_c}, \tag{22}$$

Here, ω_c is an exponential cut-off frequency corresponding to the autocorrelation relaxation time $\tau_c = 1/\omega_c$ of the medium. The friction strength $\alpha = E_r/2\hbar\omega_c$ is a dimensionless coupling constant formed by the ratio of the medium reorganization energy $E_r = (d^2/\pi)\int_0^\infty d\omega\, J(\omega)/\omega$ to twice the cut-off frequency. For a typical electron or proton transfer τ_c is in the range of 1 ps [18], while the medium reorganization energy typically exceeds $10\,\mathrm{cm}^{-1} \simeq 1.25 \times 10^{-3}\,\mathrm{eV}$.

On the other hand, for ET in polar solvents every electronic transition is accompanied by the rearrangement of a large number of molecules of the solvent leading to a spectral density of the form [6,9]

$$J(\omega) = \frac{2d^2E_r}{\pi^2\hbar c_p}\frac{\epsilon''(\omega)}{|\epsilon(\omega)|^2}, \tag{23}$$

where $\epsilon(\omega)$ is the dielectric susceptibility of the medium, and $c_p = \epsilon_\infty^{-1} - \epsilon_s^{-1}$ with ϵ_∞ and ϵ_s being the static and dielectric constants. It turns out that the reorganization energy in polar solvent is much higher as compared to rigid molecular structures. It assumes values of the order $E_r = 2000\,\mathrm{cm}^{-1} \simeq 0.25\,\mathrm{eV}$ or higher. Hence, the evaluation of the spectral density in polar media requires the experimental or theoretical knowledge of the dielectric loss function $\epsilon''(\omega)/|\epsilon(\omega)|^2$. In particular, for the case of a Debye dielectric relaxation is $\epsilon(\omega) = \epsilon_\infty + (\epsilon_s - \epsilon_\infty)/(1 - i\omega\tau_L)$, where τ_L the longitudinal dielectric relaxation time. This form yields to the dielectric loss function [7,9]

$$\frac{\epsilon''(\omega)}{|\epsilon(\omega)|^2} = \frac{c_p\omega\tau_L}{1 + (\omega\tau_L)^2}. \tag{24}$$

Hence, when $\omega \ll \tau_L^{-1}$, $J(\omega)$ has the same Ohmic linear frequency dependence as the spectral density

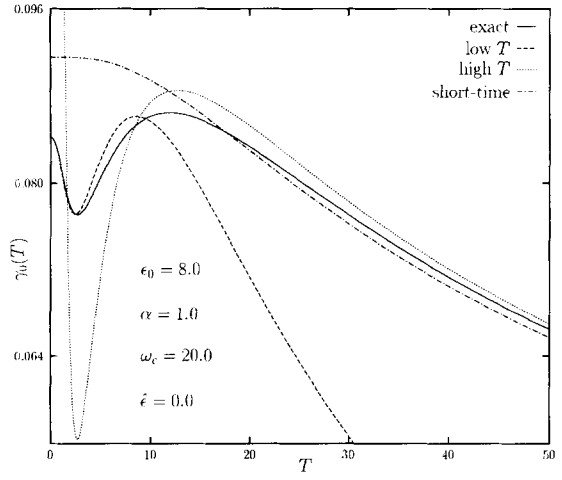

Fig. 7. The *static* rate γ_0, evaluated using the exact Eq. (25) for Ohmic friction is plotted vs. temperature T. This rate is compared with those obtained by using the low- and high-temperature approximations in Eqs. (26) and (27), as well as the short-time approximation in Eq. (31).

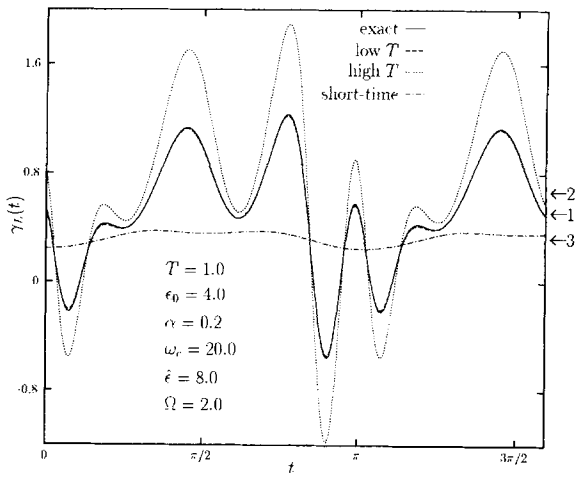

Fig. 8. The time-dependent rate $\gamma_L(t)$ for monochromatic driving in Eq. (14) is evaluated using the exact Eq. (25) for Ohmic dissipation. This rate is compared with those obtained using the short-time approximation in Eq. (31) and the low- and high-temperature approximations discussed in Eqs. (26) and (27) versus time t. In the considered regime of low temperatures T and small friction α the exact rate and the low-temperature rate coincide within line thickness. The short-time approximation loses the details of the evolution of the exact rate within a period. Finally, the arrows indicate the average value of the different rates within a period.

in Eq. (22). When $\omega \gg \tau_L^{-1}$ it decays to zero algebraically and not exponentially as in Eq. (22). In the following, we shall consider for our calculations an Ohmic spectral density of the form given in Eq. (22).

3.1. Ohmic dissipation

Inserting Eq. (22) in the definition of the bath correlation function $Q'(t)$ and $Q''(t)$ in Eq. (3), one obtains the explicit results [31]

$$Q'(t) = \alpha \ln(1 + \omega_c^2 t^2) + 4\alpha \ln\left|\frac{\Gamma(1 + 1/\hbar\beta\omega_c)}{\Gamma(1 + 1/\hbar\beta\omega_c + i\hbar/t\beta)}\right|, \quad (25)$$

$$Q''(t) = 2\alpha \arctan(\omega_c t),$$

where $\Gamma(z)$ denotes the gamma function. We stress that the above result is exact.

3.1.1. Low and high temperature approximations

In the low-temperature limit $\hbar\beta\omega_c \gg 1$ the exact result (25) reduces to the form for the Ohmic kernels usually used in the literature [12,13], with $Q''(t)$ still given by Eq. (25) and $Q'(t) \simeq Q'_L(t)$. One finds

$$Q'_L(t) = \alpha \ln(1 + \omega_c^2 t^2) + 2\alpha \ln[(\hbar\beta/\pi t)\sinh(\pi t/\hbar\beta)], \quad (26)$$

$$Q''_L(t) = Q''(t) = 2\alpha \arctan(\omega_c t).$$

On the other hand, at high temperatures $\hbar\beta\omega_c \ll 1$ the approximate expression $Q'(t) \simeq Q'_H(t)$ holds, while $Q''(t)$ still remains unchanged. We find

$$Q'_H(t) = (2\alpha/\hbar\beta\omega_c) \times [2\omega_c t \arctan(\omega_c t) - \ln(1 + \omega_c^2 t^2)], \quad (27)$$

$$Q''_H(t) = Q''(t) = 2\alpha \arctan(\omega_c t).$$

In Fig. 7 the static transfer rate γ_0 of Eq. (8), evaluated from the exact correlation functions Eq. (25), is compared with its low and high-temperature approximations. In addition, the prediction of the short-time approximation Eq. (28) discussed below is also plotted. A typical value of $\alpha = 1$ of the Ohmic strength suitable for ET reactions in condensed media is chosen, leading to a reorganization energy $E_r = 40\,\mathrm{cm}^{-1}$ if the half coupling energy $\hbar\delta$ is assumed to be $1\,\mathrm{cm}^{-1} \simeq 1.25 \times 10^{-4}\,\mathrm{eV}$. In Figs. 8

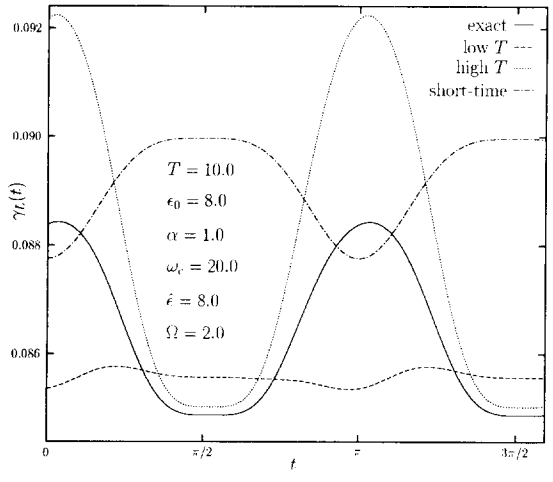

Fig. 9. As in Fig. (8), the exact time-dependent rate $\gamma_L(t)$ is compared with different approximations to it. Moderate values of the friction α and temperature T are considered. Qualitative differences are observed between the exact solution and its short-time approximation. The difference between the exact rate and the high-temperature rate is only quantitative.

and 9 the time-dependent rate $\gamma_L(t)$ (see Eq. (14)) is plotted as a function of time by using the exact solution Eq. (25) and is compared with the low and high-temperature approximations. In the regime of low temperatures and small friction considered in Fig. 8, the low-temperature approximation coincides with the exact solution within line-thickness. The high-temperature approximation deviates quantitatively, but not qualitatively, from the exact rate. In the regimes of moderate temperature and friction of Fig. 9, the low-temperature approximation is, as expected, not so good. The quantitative deviations of the high-temperature approximation from the exact one, are already within 5 per cent.

3.1.2. The short-time approximation

As discussed at the beginning of this section, in order to make quantitative predictions on the ET dynamics a suitable form for the spectral density $J(\omega)$ of the bath has to be specified. This spectral density can be either calculated from some microscopic model as in Eq. (24), or extracted for example from spectroscopic data. The crucial point is that – independent on the specific form of the spectral density $J(\omega)$ – a short-time approximation $\omega_c t \ll 1$ is commonly carried out in the ET literature [8,9,18,21,24,25,28] when performing the evaluation of the bath correlation function $Q(t)$ in Eq. (3). This approximation leads to $Q(t) \simeq Q_S(t)$ where

$$Q_S'(t) = E_r k_B T_{\rm eff} t^2/\hbar^2, \quad Q_S''(t) = E_r t/\hbar, \tag{28}$$

with $T_{\rm eff}$ being the effective temperature [8]

$$T_{\rm eff} = \frac{\hbar d^2}{2\pi k_B E_r} \int_0^\infty d\omega\, J(\omega) \coth(\hbar\omega/2k_B T). \tag{29}$$

This quantity depends on temperature and friction. At high temperatures $k_B T \gg \hbar\omega_c$ one has $T_{\rm eff} = T$, while it becomes independent on the temperature in the low-temperature limit $k_B T \ll \hbar\omega_c$. In the approximation (28), and in the absence of driving, the well known Marcus formula for the static rate $\gamma_0 = \gamma_0^{(f)} + \gamma_0^{(b)}$ of Eq. (8) is recovered, where the forward (backward) static rates $\gamma_0^{(f/b)}$ read [4,8]

$$\gamma_0^{(f/b)} = \frac{\hbar\Delta^2}{4}\left(\frac{\pi}{k_B T E_r}\right)^{1/2} e^{-(E_r \pm \epsilon_0)^2/4E_r k_B T_{\rm eff}}. \tag{30}$$

This approximation is usually thought to be appropriate whenever the reorganization energy fulfills the inequality $E_r \gg \hbar\omega_c$, being the case of ET transfer both in polar and nonpolar media. Some care has to be taken, however, because of the integration involving $Q(t)$ over *all* times, being implicit in the definition of the kernels $\hat{K}_\lambda^{(\pm)}(t)$ which enter the master equation (7), or of the relaxation rates in Eqs. (8), (14), (18) and (20). In particular, for Ohmic damping one obtains from Eqs. (28) and (29)

$$Q_S(t) = \frac{E_r \omega_c t^2}{\hbar}\left[\frac{1}{2} + \frac{\Psi'(1 + 1/\hbar\beta\omega_c)}{(\hbar\beta\omega_c)^2}\right] + \frac{iE_r t}{\hbar}, \tag{31}$$

where $\Psi'(z)$ is the derivative of the digamma function. In Fig. 7 the predictions of the short-time approximation Eq. (31) for the static rate of Eq. (8), plotted versus temperature, are compared with those of the exact result Eq. (25). In Figs. 8 and 9 the time-dependent rate $\gamma_L(t)$ of Eq. (14) is plotted as a function of time by using the exact solution Eq. (25) and the short-time approximation. Both in the regime of low temperatures and small friction considered in Fig. 8, and in that of moderate temperature and friction of Fig. 9,

the short-time rate misses the qualitative details of the evolution of the exact rate within a period. However, it improves in qualitative and quantitative agreement as the temperature is further increased (not shown).

4. Conclusions

We studied, both analytically and numerically, the asymptotic long-time dynamics of a dissipative TLS driven by monochromatic or pulse-shaped driving fields. For our calculations, a continuous Ohmic spectrum for the bath modes was considered. The asymptotic dynamics exhibits always the periodicity of the external force. The induced oscillations show a smooth periodic behavior, or a more complicate one, if, for example, multiphoton resonances at the proper frequency of the TLS occur. This resonances can be seen for strict monochromatic driving at moderately low temperatures and friction. For big static asymmetries ϵ_0 the number N of resonances observed satisfies the relation $N = \epsilon_0/\Omega$, where Ω is the driving frequency. For monochromatic driving, the oscillatory pattern becomes gradually smoothed out when the temperature, and/or the Ohmic strength are sufficiently high. It may persist, however, for pulse-shaped driving.

As it was demonstrated in [23], the dissipative and driven dynamics can always be described in terms of an exact integro-differential equation, which is non-Markovian and not invariant under continuous time-translations. An approximation to this exact equation often discussed in the literature is obtained within the NIBA approximation for the stochastic forces [20,23,28]. We compared numerically the predictions of the "exact" NIBA equation for the driven tunneling dynamics, with Markovian approximations to it often used in the literature [19–22,28]. It turns out that non-Markovian effects are usually of minor importance when the *asymptotic* tunneling dynamics is considered. Because of the complicated interplay between the stochastic and driving forces, an analysis of the time scales involved is useful to decide which is the best approximation to be considered. For example, an high frequency approximation always looses the oscillatory behaviour of the asymptotic dynamics around the averaged nonstationary population.

Finally, the bath correlation functions necessary to evaluate the Ohmic kernels appearing in the NIBA integro-differential equations were calculated exactly . We compared the predictions for the Ohmic transfer rate calculated using this exact result with the low-temperature [12,13,19,22], high-temperature and short-time approximations [8,9,18,21,28] usually used in the literature. In particular, our analysis shows that the short-time approximation, frequently used to investigate the ET dynamics, may give qualitative incorrect results at low temperatures.

Acknowledgements

MG and PH gratefully acknowledge the support of this work by the Deutsche Forschungsgemeinshaft (HA1517/14-1).

References

[1] A. Suárez and R. Silbey, J. Chem. Phys. 94 (1991) 4809.
[2] D.M. Eigler and E.K.Schweizer, Nature 344 (1990) 524; A.A. Louis and J.P. Sethna, Phys. Rev. Lett. 74 (1995) 1363.
[3] S. Han, J. Lapointe and J.E. Lukens, Phys. Rev. Lett. 66 (1991) 810.
[4] R.A. Marcus, J. Chem. Phys. 24 (1956) 966; J. Chem. Phys. 43 (1965) 679.
[5] V.G. Levich and R.R. Dogonadze, Dokl. Acad. Nauk SSSR 124 (1959) 123 [Proc. Acad. Sci. Phys. Chem. Sect. 124 (1959) 9].
[6] A.V. Ovchinnikov and M. Ya. Ovchinnikova, Zh. Eksp. Teor. Fiz. 56 (1969) 1278 [Sov. Phys. JETP 29 688 (1969)].
[7] L.D. Zusman, Chem. Phys. 49 (1980) 295.
[8] A. Garg, J.N. Onuchic and V. Ambegaokar, J. Chem. Phys. 83 (1985) 4491.
[9] I. Rips and J. Jortner, J. Chem. Phys. 87 (1987) 2090.
[10] A. Benderskii, D.E. Makarov and C.A. Wight, Adv. Chem. Phys. 88 (1994) 1.
[11] R.P. Bell, The Tunnel Effect in Chemistry (Chapman and Hall, London, 1980); E.D. German, A. M. Kuznetov and R.R. Doganadze, J. Chem. Soc. Faraday Trans. 2 76 (1980) 1128.
[12] A.J.Leggett, S. Chakravarty, A.T. Dorsey, M.P.A. Fisher, A. Garg and W. Zwerger, Rev. Mod. Phys. 59 (1987) 1.
[13] U. Weiss, Quantum Dissipative Systems, Series in Modern Condensed Matter Physics, Vol. 2 (World Scientific, Singapore, 1993).
[14] P. Hänggi, P. Talkner and M. Borkovec, Rev. Mod. Phys. 62 (1990) 251.
[15] S. Chakravarty, Phys. Rev. Lett. 49 (1982) 681; A.J. Bray and M.A. Moore, Phys. Rev. Lett 49 (1982) 1546.
[16] F. Grossmann, P. Jung, T. Dittrich and P. Hänggi, Phys. Rev. Lett. 67 (1991) 516; J.M. Gomez Llorente and J. Plata, Phys. Rev. A 45 (1992) R6958;

[17] T. Dittrich, B. Oelschlägel and P. Hänggi, Europhys. Lett. 22 (1993) 5.
[18] M. Morillo and R.I. Cukier, J. Chem. Phys. 98 (1993) 4548.
[19] M. Grifoni, M. Sassetti, J. Stockburger and U. Weiss, Phys. Rev. E 48 (1993) 3497.
[20] Yu. Dakhnovskii, Phys. Rev. B 49 4649 (1994); Ann. Phys. 230 (1994) 145.
[21] Yu. Dakhnovskii, J. Chem. Phys. 100 (1994) 6492; Yu. Dakhnovskii and R.D. Coalson, J. Chem. Phys. 103 (1995) 2908.
[22] M. Grifoni, M. Sassetti, P. Hänggi and U. Weiss, Phys. Rev. E 52 (1995) 3596.
[23] M. Grifoni, M. Sassetti and U. Weiss, Phys. Rev. E 53 (1996) R2033.
[24] D.G. Evans, R.D. Coalson, H.J. Kim and Y. Dakhnovskii, Phys. Rev. Lett. 75 (1995) 3649.
[25] D.G. Evans, R.D. Coalson and Y. Dakhnovskii, J. Chem. Phys. 104 (1996) 2287.
[26] R. Löfstedt and S.N. Coppersmith, Phys. Rev. Lett. 72 (1994) 1947; M. Grifoni and P. Hänggi, Phys. Rev. Lett. 76 (1996) 1611.
[27] D.E. Makarov and N. Makri, Phys. Rev. B 52 (1995) R2257.
[28] I.A. Goychuk, E.G.Petrov and V. May, Chem. Phys. Lett. 353 (1996) 428.
[29] M. Grifoni, Phys. Rev. E 54 (1996) R3086.
[30] C. Aslangul, N. Pottier and D. Saint-James, Phys. Lett. A 110 (1985) 249; J. Phys. (Paris) 47 (1986) 1657.
[31] R. Egger and U. Weiss, Z. Phys. B 89 (1992) 97.

Reprinted from

Chemical Physics

Chemical Physics 232 (1998) 371–372

Erratum

Erratum to "Dissipative tunneling with periodic polychromatic driving: Exact results and tractable approximations" [Chem. Phys. 217 (1997) 167] [1]

Milena Grifoni, Ludwig Hartmann, Peter Hänggi *

Institut für Physik, Universität Augsburg, Memminger Strasse 6, 86135 Augsburg, Germany

Accepted 12 March 1998

ELSEVIER

ELSEVIER

Chemical Physics 232 (1998) 371–372

Chemical Physics

Erratum

Erratum to "Dissipative tunneling with periodic polychromatic driving: Exact results and tractable approximations" [Chem. Phys. 217 (1997) 167] [1]

Milena Grifoni, Ludwig Hartmann, Peter Hänggi *

Institut für Physik, Universität Augsburg, Memminger Strasse 6, 86135 Augsburg, Germany

Accepted 12 March 1998

Four changes need to be made to the original article.

(i) The r.h.s. of Eq. (3) should be multiplied by $\hbar^{-1}$.

(ii) The text starting on the first line of page 172 after citation of Refs. [19,22], and ending with Eq. (15), should be substituted by the following paragraph:

As the frequency is increased, the λ dependence of the kernels $\hat{K}_{\lambda}^{(\pm)}(t)$ cannot be anymore neglected. Though, as long as τ_K remains the *shortest* time scale of the problem, a Markovian approximation to the generalized master equation (4) can still be invoked. Let us next define $\gamma_{\rm L}(t) := \Sigma_m e^{-im\Omega_p t} k_m^+(-im\Omega_p)$, and $\rho_{\rm L}(t) := \mathscr{F}(t)$, cf. Eq. (12). Then, the Markovian approximation to the integro-differential equation (4) reads

$$\dot{P}_{\rm L} = -\gamma_{\rm L}(t)\left[P_{\rm L}(t) - P_{{\rm L},ns}(t)\right], \tag{1}$$

with time-dependent rate explicitly given by

$$\gamma_{\rm L}(t) = \int_0^{\infty} {\rm d}\tau h^{(+)}(\tau)\cos\left[\zeta(t, t-\tau)\right], \tag{2}$$

and time-dependent nonstationary equilibrium value $P_{{\rm L},ns} = \rho_{\rm L}(t)/\gamma_{\rm L}(t)$, where

$$\rho_{\rm L}(t) = \int_0^{\infty} {\rm d}\tau h^{(-)}(\tau)\sin\left[\zeta(t, t-\tau)\right]. \tag{3}$$

Eqs. (1), (2) and (3) above should substitute Eqs. (13), (14) and (15), respectively. The results shown in Fig. 4 where obtained with the above expressions for the functions $\gamma_{\rm L}$ and $\rho_{\rm L}$.

* Corresponding author.

[1] PII of original article: S0301-0104(97)00020-7.

PII: S0301-0104(98)00120-7

(iii) The validity of the high frequency approximation for monochromatic driving should be modified as $\Omega_p \gg \gamma_H$, Δ, where γ_H denotes the high frequency rate in Eq. (18).

Correspondingly, the validity of the low Ω_p + high Ω approximation discussed for pulse-shaped periodic driving requires $\tau_K^{-1} \gg \Omega \gg \gamma_H \gg \{\Omega_p, \Delta\}$.

(iv) $Q'(t)$ in Eq. (25) should read

$$Q'(t) = \alpha \ln\left(1 + \omega_c^2 t^2\right) + 4\alpha \ln\left|\frac{\Gamma(1 + 1/\hbar\beta\omega_c)}{\Gamma(1 + 1/\hbar\beta\omega_c + it/\hbar\beta)}\right|. \quad (4)$$